Ligand Specificity and Affinity in the Sulforhodamine B Binding RNA Aptamer

Kyle Piccolo[a], Brooke McNeil[a], Jeff Crouse[b], Su Ji Lim[b], Sarah C. Bickers[a], W. Scott Hopkins[b] & Thorsten Dieckmann[a]*.

[a]Department of Chemistry, University of Waterloo, 200 University Avenue West, Waterloo, ON N2L 3G1

[b]Waterloo Institute for Nanotechnology, University of Waterloo, 200 University Avenue West, Waterloo, ON, N2L 3G1

*To whom correspondence should be addressed:

Dr. Thorsten Dieckmann: thorsten.dieckmann@uwaterloo.ca (Tel. 1-519-888-4567 ext. 35036)

Abstract

Binding affinity and selectivity are critical properties of aptamers that must be optimized for any application. The sulforhodamine B binding RNA aptamer (SRB-2) is a somewhat promiscuous aptamer that can bind ligands that vary markedly in shape, size and charge. Here we categorize potential ligands based on their binding mode and structural characteristics required for high affinity and selectivity. Several known and potential ligands of SRB-2 were screened for binding affinity using LSPR, ITC and NMR spectroscopy. The study shows that rhodamine B has the ideal structural and electrostatic properties for selective and high-affinity binding of the SRB-2 aptamer.

Keywords: SRB-2, Aptamer, Ligand, Binding affinity, Selectivity

List of Abbreviations

9AA, 9-aminoacridine; AO, acridine orange; AR101-B, Atto rhodamine 101 biotin; B-TMR, biocytin tetramethyl rhodamine; FL, fluorescein; MG, malachite green; PBV, Patent blue V; PY, pyronin Y; RB, rhodamine B; SR, sulforhodamine B; SR101, sulforhodamine 101; SRB-2, sulforhodamine B RNA aptamer; TMR, tetramethylrosamine; XC, xylene cyanol FF

1.0 Introduction

Aptamers are RNA, DNA or modified oligonucleotides selected to bind a target with high affinity and selectivity[1,2]using a process termed SELEX (systematic evolution of ligands by exponential enrichment). The sulforhodamine B binding aptamer (SRB-2) is an RNA aptamer selected to bind the fluorescent dye sulforhodamine B (SR)[3]. The secondary structure of the RNA and the structures of six ligands are shown in Figure 1. Some of the very first targets used in the development of SELEX were small, organic, planar fluorophores due to their similarity to biological cofactors and comparatively high quantum yield[2]. Such aptamers, including SRB-2, continue to be widely studied due to their potential applications in bio-imaging and bio-sensing[4–7]. SRB-2 is an intriguing system due to the negative charge of its ligand, SR. Negatively charged aptamer ligands are less common than neutral and positively charged ones due to potentially repulsive backbone interactions. SRB-2 can bind a variety of planar dyes which contain a similar characteristic xanthene ring structure. These dyes are diverse in colour, size, charge and selectivity. Many of these ligands are some type of rhodamine derivative. SRB-2 is also capable of binding the propeller-shaped dye Patent Blue V(PBV), albeit with lower affinity [8]. Here we utilize these ligands to probe the structure of SRB-2. Characterizing aptamer systems such as SRB-2 is essential to rationalize the motifs and intermolecular contacts that are critical for binding affinity and specificity.

The SRB-2 aptamer was selected to use it in so-called “light-up” RNA aptamer systems[3]. This is a promising method wherein the complement of a fluorophore binding aptamer sequence is added to a gene of interest. The target fluorophores have low intrinsic fluorescence but become highly fluorescent

upon binding the aptamer[6,9]. Several other fluorophore binding aptamers, particularly the class based on derivatives of the GFP fluorophore such as spinach[10] and broccoli[11], have been selected and studied to create a rainbow of RNA reporter molecules for nucleic acid researchers analogous to the arsenal of fluorescent proteins used by protein researchers[9,12]. SRB-2 has been used successfully in mRNA imaging experiments with SR and with SR-quencher constructs designed to reduce background noise in fluorescence measurements[4,5]. Ligand analogues have been studied as well, some of which have higher fluorescence enhancement, but bind by non-specific intercalation,limiting their practical use[5]. Recently, a solution structure of an aptamer selected for the related dye tetramethylrhodamine was determined[13].

Here we use a variety of biophysical techniques to characterize and compare kinetics and binding mode of several aptamer-ligand complexes of SRB-2. Fluorescence and isothermal titration calorimetry (ITC) are used to probe binding affinity and selectivity of known and potential ligands. Thermodynamic parameters of selective binders are also assessed via ITC. RNA-ligand interactions are examined through the use of nuclear magnetic resonance (NMR) spectroscopy.

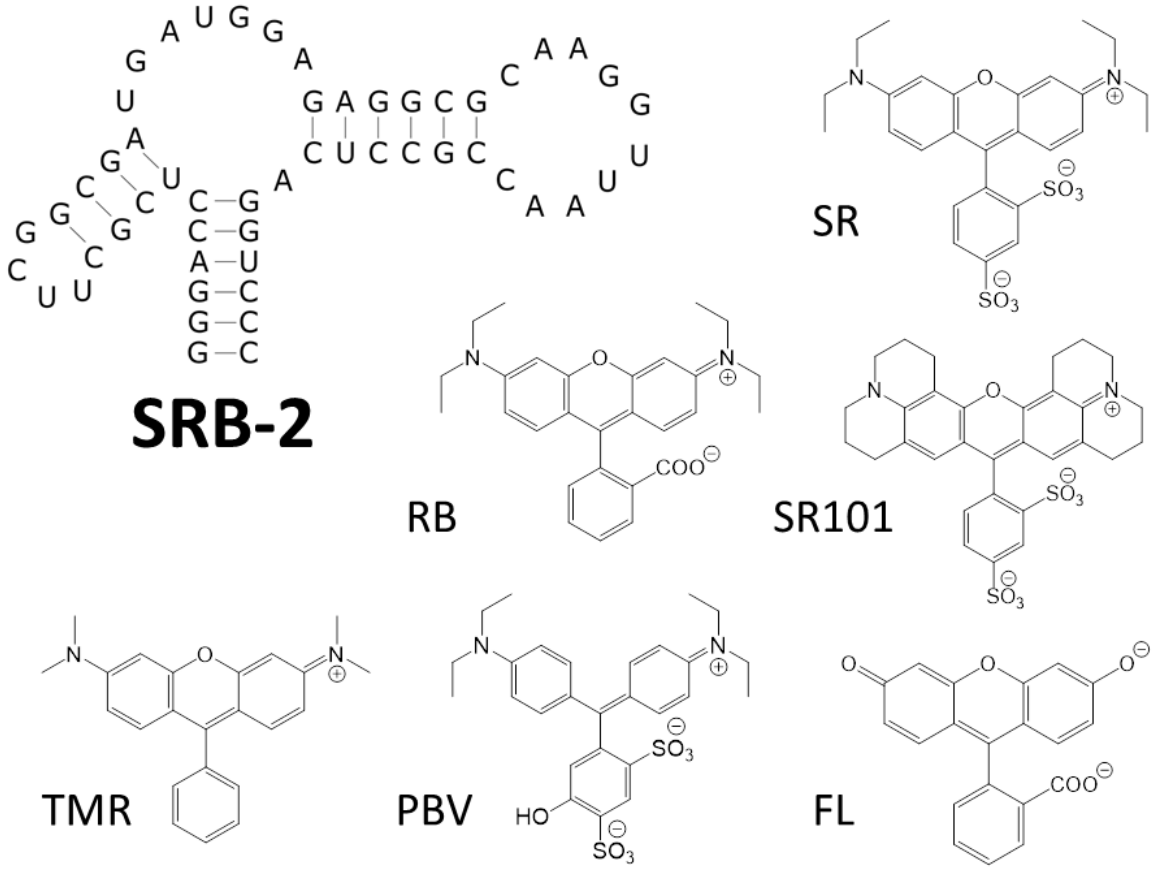

Figure 1: Secondary structure of SRB-2 and chemical structures of several studied dyes. Chemical structures of all other dyes discussed can be found in Figure S1.

2.0 Experimental Methods

2.1 Preparation of RNA Samples and Dyes

The SRB-2 RNA was synthesized enzymatically using a T7 RNA polymerase and double-stranded synthetic DNA template (5'GGGACCTGAGGCGGTTAACCTTGCGCCTCTCC ATCATCGCCGAAGCGAGGTCCCTATAGTGAGTCGTATTA-3'). A single base-pair substitution in the original sequence (A3 –> G3 and U52 –> C52) was introduced to increase transcriptional yield[14,15]. The RNA was purified on a 10% Urea PAGE gel followed by clean-up on a HiPrep 16/10 DEAE FF anion-exchange column (GE Healthcare, Uppsala, Sweden), and desalting on a HiPrep 26/10 Desalting column (GE Healthcare, Uppsala, Sweden). The samples were then lyophilized and dissolved in the appropriate buffer.

Sulforhodamine B (Life Technologies, Eugene, OR), sulforhodamine 101, acridine orange, 9-aminoacridine, Atto 495, rhodamine 110 chloride, fluorescein (Sigma, St. Louis, MO), rhodamine B, rhodamine 6G (Alfa Aesar, Ward Hill, MA), tetramethylrosamine (Invitrogen Corporation, Carlsbad, CA), pyronin Y (Acros Organics, Geel, Belgium) and xylene cyanol FF (EMD, Burlington, MA) were used without further purification. Dyes were dissolved in water to prepare stock solutions, and concentrations were verified by UV/vis spectrophotometry.

2.2 Emission Scans

Spectra were obtained using a Spectramax M3 Multi-Mode Microplate Reader using a 100 nm wide scan with 1nm intervals in an appropriate range based on literature maximum emission wavelengths. Samples were prepared with 10µM dye and 50µM RNA in assay buffer (10mM HEPES, 10mM KCl and 5mM $MgCl_2$ at pH 7.4). Sequences can be found in the supplementary information.

2.3 ITC Studies

Experiments were performed at 25 °C on a MicroCal ITC 200 microcalorimeter (MicroCal Inc., Northampton, MA). The samples of 30-35 µM RNA and dye solutions of 0.7-1.1 mM were each prepared by dissolving in assay buffer. All experiments were carried out at 25°C and performed in triplicate. A blank run with buffer in the cell and fluorophore in the syringe was performed and subtracted from the experimental run to account for heat of dilution of the fluorophore solutions. All data sets were analyzed and fitted using the Origin 7 software package provided by MicroCal. All data was fit to a single-site binding model using a non-linear least-squares approach.

2.4 LSPR Assay

Localized surface plasmon resonance (LSPR) binding assays were carried out on an OpenSPR™ (Nicoya, Waterloo, Canada) at room temperature. For the analysis of SRB-2, 10µM biocytin TMR

(Invitrogen Corporation, Carlsbad, CA) or biotinylated Atto Rho101 (Sigma, St. Louis, MO) were immobilized onto the streptavidin sensor chip. SRB-2 was then injected at a flow rate of 20 µL/min at concentrations of 0.9 – 7.57 µM in HEPES (10 mM HEPES, 200 mM KCl, 10 mM $MgCl_2$) running buffer. The binding time was 240 seconds, and the disassociation time was 150 seconds. The sensor was regenerated with 10 mM glycine-HCl (pH 2.5). The data was retrieved and analyzed with TraceDrawer software (Ridgeview Instruments AB, Sweden). A 1:1 Langmuir interaction was fit to the data for each compound, and the fit delivered the association constant (k_a), dissociation constant (k_d), and the equilibrium constant (K_D).

2.5 NMR Experiments

All spectra were collected on a Bruker DRX-600 spectrometer equipped with an HCN triple-resonance, triple-axis PFG probe using established techniques [16]. Quadrature detection for the indirect dimensions in multidimensional experiments was achieved using the States-TPPI method. Samples in 90% H_2O/10% D_2O that were used to observe exchangeable protons were run using 1-1-spin echo solvent suppression. Two-dimensional NOESYspectra in 90% H_2O/10% D_2O were acquired at 277 K with a mixing time of 150 ms. Samples in D_2O (Cambridge Isotopes) that were used to observe non-exchangeable protons were run with presaturation solvent suppression. 2D CITY-TOCSY with a mixing time of 50 ms, and NOESY with a mixing time of 150 ms in 100% D_2O were acquired at 298 K. All NMR samples were 500 µL in standard 5 mm NMR tubes.

2.6 Electrostatic Potential Surfaces

All electrostatic potential surface (EPS) calculations were performed using the Gaussian 16 program package for computational chemistry. The molecules were optimized at B3LYP/def2-TZVPP level of theory, besides Atto Rhodamine 101, 6-Biocytin TMR, and Patent Blue V, which were optimized at B3LYP/def2-SVP level. Frequency calculations were performed to ensure that structures are at its minima and not at a transition state.

3.0 Results

3.1 Emission Scans

Fluorescence emission spectra were obtained for each dye both on their own and bound to SRB-2 in an 8:1 ratio. The specificity of these dyes was tested using additional RNA and dsDNA sequences. Dyes that could bind SRB-2 only included sulforhodamine B (SR), rhodamine B (RB) and sulforhodamine 101 (SR101), as well as 5/6-biocytin tetramethylrhodamine (B-TMR) and Atto rhodamine 101 biotin (AR101-B), which are functionalized analogues of RB and SR101, respectively. All other dyes listed were capable of binding all sequences tested. Most dyes experienced a red shift in their maximum emission wavelength and an increase in fluorescence upon binding.

.As shown in Table 1, 9-aminoacridine (9AA) and acridine orange (AO) are exceptions, likely a result of a pKa change in the amines which alters their protonation state.

Table 1: Wavelength shifts and fluorescence changes determined by emission scans

Oligonucleotide		SR	RB	TMR	PyrY	SR101	B-TMR	AR101-B	AO	Atto	9AA
Assay buffer	RF	1.00	1.00	1.00	1.00	1.00	1.00	1.00	1.00	1.00	1.00
	λmax(nm)	580	576	573	563	604	578	605	526	516	435
SRB-2	RF	1.26	1.48	0.87	0.92	0.85	0.90	1.11	2.99	3.32	0.21
	Δλmax(nm)	8	6	10	9	4	8	1	-2	11	0
dsDNA template	RF	0.91	0.80	0.35	0.28	0.63	0.83	0.84	2.39	2.53	0.19
	Δλmax(nm)	-2	0	9	9	0	1	2	-1	7	0
MG aptamer	RF	0.87	0.78	0.37	0.28	0.89	0.83	0.92	2.90	2.50	0.26
	Δλmax(nm)	-1	0	6	9	0	2	1	-3	10	0
Mango aptamer	RF	0.92	0.79	0.30	0.94	0.74	0.73	0.78	1.94	3.29	0.37
	Δλmax	-2	0	9	9	1	1	3	1	12	0

Relative fluorescence (RF) values are calculated as a normalized ratio of fluorescence observed by each fluorophore in the presence of indicated oligonucleotide versus in buffer only.

3.2 Isothermal Titration Calorimetry

Isothermal titration calorimetry (ITC) was used to determine the binding affinity of the ligands, and is given in Table 2. Through the dissociation constant, K_d, we find the order of binding affinities to SRB-2 is RB > SR101 > SR. The binding of ligands to aptamers is commonly dependent on divalent counter-ions for stabilization of the negatively charged backbone. To probe this relationship, the ITC experiments were repeated in the absence of Mg^{2+}. No binding was observed under these conditions for SR, SR101 or RB. Weak binding was observed for TMR, which carries an overall positive charge. ITC experiments at 500mM KCl in the absence of Mg^{2+} showed weak binding of the dye ligands to SRB-2 which indicates that monovalent cations at high concentrations can stabilize the SRB-2 aptamer and allow ligand binding, albeit less effectively.

Several other dyes, including tetramethyl rosamine (TMR), pyronin Y (PY), Atto 495, AO and 9AA were tested by ITC. However, these small, planar and electron-poor dyes intercalate between base pairs in double-stranded nucleic acid sequences. The resulting isotherms adhered poorly to a single-site binding model. Therefore reasonable binding affinities and thermodynamic parameters were not determined by this method. PY, AO, 9AA and Atto 495 also mirror the trend observed in previous studies using fluorescence titrations[5].

Table 2: Thermodynamic parameters of SRB-2 determined by ITC

Ligand	*n*	K_d (µM)	ΔH (kcal mol^{-1})	ΔS (cal mol^{-1} K^{-1})
SR	0.885 ± 0.012	1.45 ± 0.09	-13.1 ± 0.3	-17.2 ± 0.4
SR101	0.882 ± 0.031	4.7 ± 0.70	-10.1 ± 0.5	-9.27 ± 0.8
RB	0.922 ± 0.010	0.447 ± 0.08	-14.2 ± 0.2	-18.5 ± 1.2

3.3 Surface Plasmon Resonance Studies

LSPR anisotropy experiments were performed in order to obtain kinetic data for the structurally relevant rhodamine deratives biocytin-tetramethyl rhodamine (B-TMR) and Atto rhodamine 101 biotin. These dyes were selected based on commercial availability and ability to bind the surface of SPR chips. Binding data obtained for these dyes is listed in Table 3.

Table 3: Kinetic parameters of SRB-2 binding determined by LSPR

Ligand	k_a (uM^{-1} s^{-1})	k_d (s^{-1})	K_D (uM)
B-TMR	207 $\pm$ 78.0	0.0292 $\pm$ 0.0156	1.37 $\pm$ 0.23
AR101-B	735 $\pm$ 559	0.0246 $\pm$ 0.0346	4.66 $\pm$ 0.47

3.4 NMR Spectroscopy

The binding behavior of SRB-2 with each ligandwas studied by NMR spectroscopy. SRB-2 was titrated with each ligand in 3-5 steps. 1D ^{1}H-NMR spectra in 90% H_2O/10% D_2O were used to follow the changes during the titrations. The spectrum of SRB-2 in the absence of dye shows relatively few and generally broad peaks (Figure 2A). This is typical for the adaptive binding mode found in many aptamers[17,18], where the binding pocket in the absence of ligand is mostly unstructured. When the aptamer has been titrated to approximately 1:1 with each of the ligands (Figure 2B-E), an NMR spectrum consistent with a single conformation is observed. This is indicated by the presence of additional peaks compared to the spectrum of the free SRB-2 andlinewidths that are noticeably narrower. Several of the new peaks are in the region from 9-11 ppm, which is typical for imino protons in non-canonical base pairs. Narrower line shapes in the NMR spectrum and additional peaks in the 9-11 ppm region is consistent with a more highly structured bound conformation with more contacts forming between the imino protons of guanine or uridine residues and other atoms in the aptamer or ligand.

TOCSY experiments were run on SRB-2complexed with SR, RB and SR101. The aromatic protons of the ligands, particularly those on the single rings, are shifted downfield when bound to SRB-2 as a result of diamagnetic anisotropy experienced by these aromatic protons when they are involved in π-π stacking interactions with bases of the aptamer. It was qualitatively observed in these spectra that RB

protons have a larger change in the chemical shift between free and bound forms ($\Delta\delta_{free\text{-}bound}=\delta_{free}-\delta_{bound}$) as compared with SR, which shows larger shifts as compared with SR101.

NOESY experiments in 90% H_2O/10% D_2O are used to map interactions between imino-protons. The NOEs between exchangeable imino protons in adjacent base-pairs allow a comparison of the patterns formed in the unfolded and folded states of the aptamer. SR has the greatest number of NOEs between exchangeable protons. This is expected as SR was the ligand SRB-2 was initially selected to bind, so the binding site is optimized for this molecule. The NOESY spectrum for RB is almost identical to SR, except for some minor chemical shift changes. In the SR101 spectrum, fewer imino to imino stacking NOEs are present as compared to the spectrum for SR. In the NOESY spectrum of TMR, even fewer stacking NOEs are present when compared to SR. In addition, no clear transition to a single conformation was observed based on the changes in the 1D ^{1}H-NMR spectra (Figure 2E). This suggests that TMR may not be inducing the same conformation of the aptamer, consistent with all previous data. PY, AO, 9AA and Atto 495 all have similar spectra to TMR, where only signals from known Watson-Crick base pairs in the stem regions are observed. This suggests that all these dyes intercalate in the base-paired stems, rather than participating in adaptive aptamer binding.

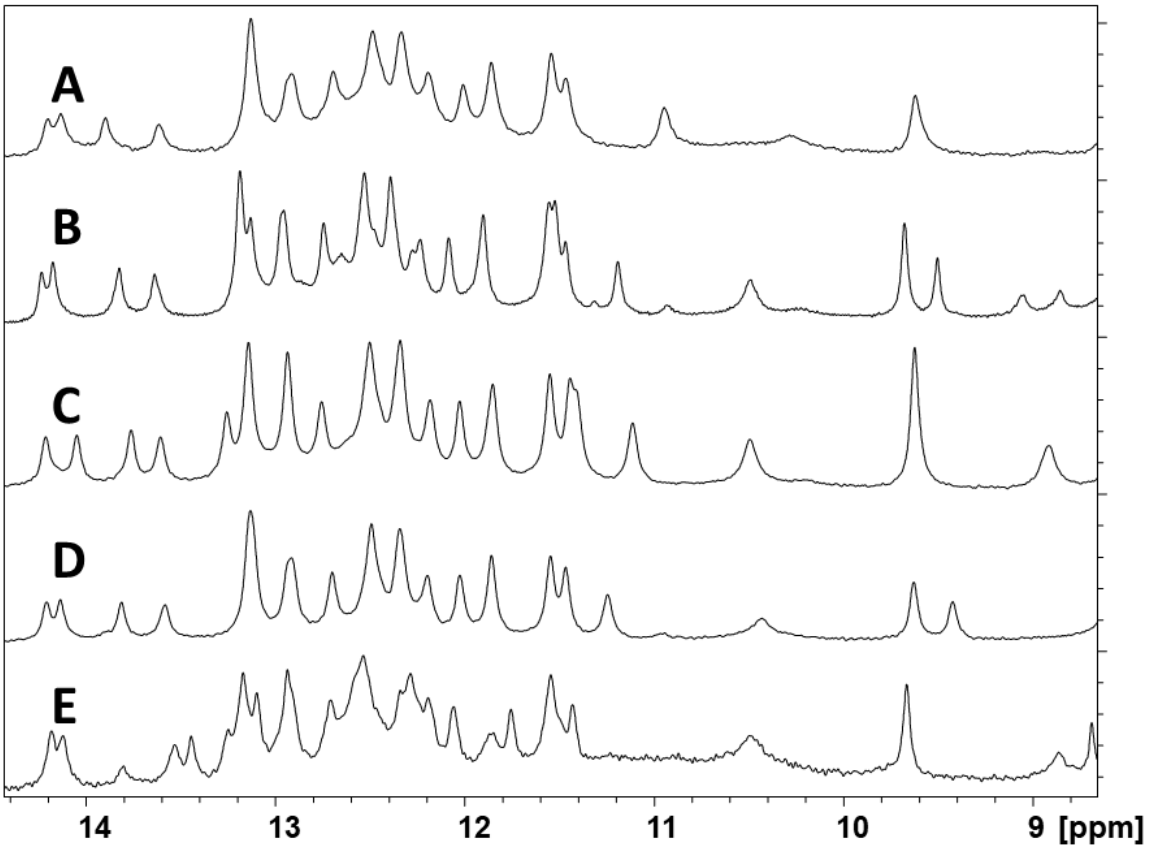

Figure 2: 1D ^{1}H NMR spectra of free SRB-2 and SRB-2 bound in a 1:1 ratio to several different ligands. A) 0.9 mM SRB-2 only B) 1.8 mM SR, C) 1.3 mM RB, D) 1.1 mM SR101, E) 0.4 mM TMR.

4.0 Discussion

4.1 Smaller size and reduced negative charge result in higher binding affinity

From the emission scans , we show that RB has a similar red shift but greater fluorescence intensity increase than SR (Table 1) when binding to SRB-2. A comparable red shift is expected due to their conjugation systems being very similar. The fluorescence intensity increase for RB binding is likely higher as compared with SR due to differences in the polarity of the bound dyes. RB is missing a negatively charged group in the para-position of the single ring, which results in the ligand's conformation being locked more tightly in the binding site. Figure 3 shows that the negatively charged sulfonates in SR draw electron density from the three-ring system, creating a significant concentration of negative partial charge on the bottom ring. RB has a single carboxyl group rather than two sulfonate groups. The carboxyl group of RB is smaller and less electron-dense than the sulfonates on SR, resulting in a dye with less overall electron density. The reduction in repulsive interactions with the RNA backbone and the size of groups on the extended ring would account for the small relative increase in enthalpy and entropy, respectively. It also makes sense that RB would have a lower K_D for SRB-2 because the original selection target had a PEG-anchor at the para position rather than a negative charge and therefore possessed an overall neutral charge like RB. The NMR spectra support this as only minor chemical shift changes are observed between the two complexes.

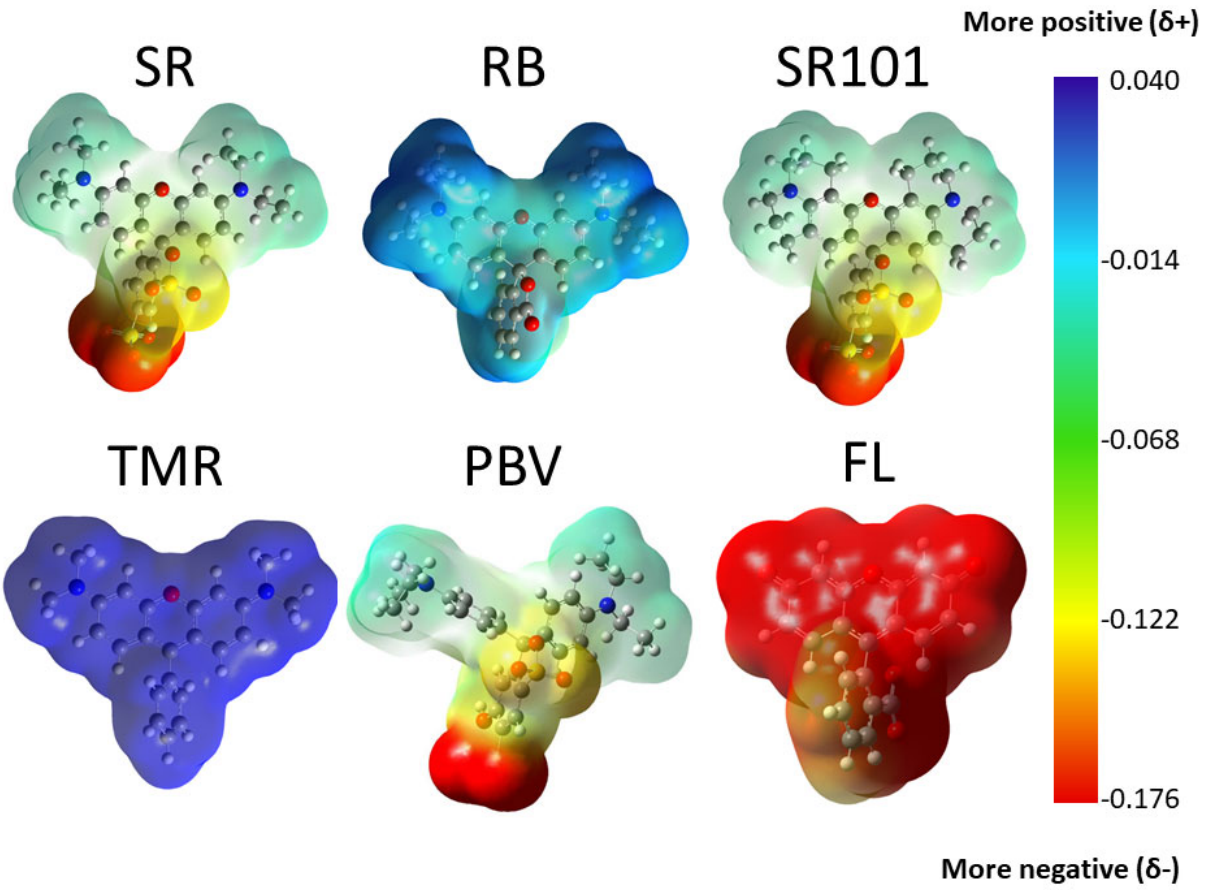

Figure 3: Electrostatic potential surfaces (EPS) for five SRB-2 ligands and the counter-selection target, fluorescein. The upper charge limit was set by averaging the maximum positive charges in all ligands calculated. The lower charge limit was set by averaging the minimum negative charges in all ligands calculated and subtracting one standard deviation.

It can also be observed from the fluorescence data in Table 1 that SR101 has a similar fluorescence increase but a smaller red shift compared to SR. The smaller red shift results from SR101 being more rigid in its free conformation. This would fit with the ITC results in Table 2 which indicate that the entropy loss upon binding is relatively small for SR 101. This is in agreement with the observed K_D values as SR101 is expectedly higher than SR as the tighter the binding pocket, the stronger the π-π stacking interactions will be, resulting in a larger fluorescence redshift. There is also a significant decrease in the entropy loss of SR101 compared to SR. This decrease in entropy loss can be attributed to SR101 having a more rigid ring structure in place of the freely rotating ethyl groups in SR, the more ordered structure resultsin a smaller entropy loss upon binding. The enthalpy change for SR101 binding is also smaller compared to SR, which can also be explained by the steric interactions between the bulkier rings, resulting in less ideal π-π stacking with the xanthene ring structure of the dye. NOESY

experiments indicate that the aptamer is unable to form some contacts with SR101 that are observed with SR and RB, indicating that SR101 doesn't fit as well in the aptamer binding pocket.

4.2 Negatively charged group is required for selectivity but is likely not directly involved in binding

TMR binding to SRB-2 resulted in the most significant chemical shift changes in the TOCSY spectrum as compared to SR binding. However, even with significant over-titration, multiple conformations appear to be present based on the number of H5-H6 crosspeaks observed. There are also fewer NOEs observed in the SRB-2/TMR NOESY spectrum than in the SRB-2/SR spectrum, indicating that TMR is not inducing the formation of a specific binding pocket at all. TMR is known, from studies with MGA, to intercalate between base pairs of double-stranded RNA[19]. Similar observations were made for PY, AO, 9AA and Atto 495. Overall, this suggests that all of these small, positively charged dyes intercalate rather than participate in specific adaptive aptamer binding. These observations also indicate that selective binding of SRB-2 is only possible in the presence of a negatively charged ring well.

SR101 and AR101-B differ slightly in that the para sulfonate is replaced by biotin, and the other is missing entirely. Little difference is observed in the K_D for complexation with SRB-2 between these two dyes, despite a marked change in the electrostatic potential map. This suggests that the negative charge often found in the ortho position of these dyes plays no significant role in binding and likely interacts mostly with solvent, similar to the phosphate groups of ATP when bound to the ATP aptamer[20]. Aside from the biocytin group, B-TMR and SR differ in that B-TMR has a carboxyl group instead of a sulfonate on the single ring and diaminomethyl groups in place of diaminoethyl groups. Based on the SRB-2 binding observations with AR101-B and SR101, the difference in charged groups is expected to have little impact. However, despite B-TMR being more structurally similar to RB, the K_D for complexation with SRB-2 is more similar to that found for SR . This is likely due to the presence of the smaller methyl groups in B-TMR versus ethyl groups in SR.

4.3 Size and shape of the alkyl groups is crucial for binding

Concerning the nature of these alkyl groups, the SRB-2 aptamer has specific requirements. Fluorescein was used in a counter selection step during SELEX[3], resulting in the removal of sequences capable of binding to a dye with electron-withdrawing oxygens, rather than the tertiary amines found in SR. The resulting consensus sequence would be expected to have electrostatic interactions with the RNA backbone preventing the correct folding of the aptamer in this case. Dyes such as Xylene cyanol FF (XC) and Patent Blue V (PBV) are missing the bridging oxygen in the middle ring, resulting in a propeller-like structure, rather than a planar structure. It is probable then that stacking interactions are much less ideal in this case due to its freedom of mobility, and steric hindrance by the additional methyl groups adjacent to the aminoethyl groups. Interestingly, PBV has been shown to bind SRB-2 weakly[8], indicating a molecule of this shape can fit in the SRB-2 binding site. However, XC cannot bind, and the only difference is that PBV has the traditional diaminoethyl groups while XC has aminoethyl groups,

which are secondary amines. Rhodamine 6G has the same aminoethyl groups as XC and also cannot bind, despite being planar like SR. Rhodamine 110 has primary amines and likewise is unable to bind. This suggests that, despite the similarities in electron density, SRB-2 is selective for tertiary amine groups. This fact indicates that with respect to SR101, the steric hindrance of the bulky ring groups is the limiting factor in binding, likely preventing the aptamer from coming in close enough contact to the negative charges for them to have an effect on binding affinity. Supporting this idea are the association and dissociation rates also obtained in LSPR experiments. As seen in Table 3, the difference in binding constant between TMR-B and AR101-B clearly comes from the association rate. The aptamer's structure has to adapt and strain further to allow AR101-B to bind compared to TMR-B, resulting in a slower rate of binding. The ligands are released by the aptamer at a comparable rate due to their relative similarity in charge distribution.

5.0 Conclusion

In summary, we have shown that an ideal ligand for SRB-2 has several requirements. For optimal binding affinity, the amine groups must have small alkyl constituents that are able to participate in hydrophobic interactions but are not so large as to interfere with the aptamer's binding conformation. The absence of a negative charge in the para position on the single ring also contributes positively to binding affinity. A negatively charged group on the ortho position has little impact on binding affinity but is required for selective binding of SRB-2 as repulsive interactions with the RNA backbone prevent these ligands from intercalating in base paired regions of the aptamer. As observed with AR101-B, bulky amine constituents can also confer selective binding of SRB-2 in the absence of this negative charge but at a considerable loss of binding affinity. Taking these observations into account, rhodamine B was shown to be the SRB-2 ligand with the best properties among those tested.

Declaration of competing interest

The authors declare no competing financial interests.

Acknowledgements

We thank Ms. Maryam Najib and Ms. Dami Adebajo for their help with sample preparation. This work was supported by the Natural Sciences and Engineering Research Council (NSERC) via Discovery Grants (TD and WSH), and a Collaborative Research and Development Grant (WSH).

References

[1] C. Tuerk, L. Gold, Systematic evolution of ligands by exponential enrichment: RNA ligands to bacteriophage T4 DNA polymerase, Science (80-.). 249 (1990) 505–510.

https://doi.org/10.1126/science.2200121.

[2] A.D. Ellington, J.W. Szostak, In vitro selection of RNA molecules that bind specific ligands, Nature. 346 (1990) 818–822. https://doi.org/10.1038/346818a0.

[3] L.A. Holeman, S.L. Robinson, J.W. Szostak, C. Wilson, Isolation and characterization of fluorophore-binding RNA aptamers, Fold. Des. 3 (1998) 423–431. https://doi.org/10.1016/S1359-0278(98)00059-5.

[4] A. Arora, M. Sunbul, A.J.¨ Aschke, Dual-colour imaging of RNAs using quencher-and fluorophore-binding aptamers, Nucleic Acids Res. 43 (2015). https://doi.org/10.1093/nar/gkv718.

[5] M. Sunbul, A.J.¨ Aschke, SRB-2: a promiscuous rainbow aptamer for live-cell RNA imaging, Nucleic Acids Res. 46 (2018). https://doi.org/10.1093/nar/gky543.

[6] F. Bouhedda, A. Autour, M. Ryckelynck, Light-up RNA aptamers and their cognate fluorogens: From their development to their applications, Int. J. Mol. Sci. 19 (2018). https://doi.org/10.3390/ijms19010044.

[7] W. Xu, Y. Lu, Label-free fluorescent aptamer sensor based on regulation of malachite green fluorescence, Anal. Chem. 82 (2010) 574–578. https://doi.org/10.1021/ac9018473.

[8] J.R. Babendure, S.R. Adams, R.Y. Tsien, Aptamers Switch on Fluorescence of Triphenylmethane Dyes, J. Am. Chem. Soc. 125 (2003) 14716–14717. https://doi.org/10.1021/ja037994o.

[9] J. Ouellet, RNA fluorescence with light-Up aptamers, Front. Chem. 4 (2016). https://doi.org/10.3389/fchem.2016.00029.

[10] J.S. Paige, K.Y. Wu, S.R. Jaffrey, RNA mimics of green fluorescent protein, Science (80-.). 333 (2011) 642–646. https://doi.org/10.1126/science.1207339.

[11] G.S. Filonov, J.D. Moon, N. Svensen, S.R. Jaffrey, Broccoli: Rapid selection of an RNA mimic of green fluorescent protein by fluorescence-based selection and directed evolution, J. Am. Chem. Soc. 136 (2014) 16299–16308. https://doi.org/10.1021/ja508478x.

[12] S. Neubacher, S. Hennig, RNA Structure and Cellular Applications of Fluorescent Light-Up Aptamers, Angew. Chemie - Int. Ed. 58 (2019) 1266–1279. https://doi.org/10.1002/anie.201806482.

[13] E. Duchardt-Ferner, M. Juen, B. Bourgeois, T. Madl, C. Kreutz, O. Ohlenschlager, J. Wohnert, Structure of an RNA aptamer in complex with the fluorophore tetramethylrhodamine, Nucleic Acids Res. 48 (2020) 949–961.

[14] J.F. Milligan, D.R. Groebe, G.W. Witherell, O.C. Uhlenbeck, Oligoribonucleotide synthesis using T7 RNA polymerase and synthetic DNA templates, Nucleic Acids Res. 15 (1987) 8783–8798. https://doi.org/10.1093/nar/15.21.8783.

[15] J.F. Milligan, O.C. Uhlenbeck, Synthesis of small RNAs using T7 RNA polymerase, Methods Enzymol. 180 (1989) 51–62. https://doi.org/10.1016/0076-6879(89)80091-6.

[16] T. Dieckmann, M. Piazza, E. Bonneau, P. Legault, Biomolecular NMR Spectroscopy of Ribonucleic Acids, in: ELS, John Wiley & Sons, Ltd, Chichester, UK, 2014.

https://doi.org/10.1002/9780470015902.a0021033.pub2.

[17] J.B. Da Costa, A.I. Andreiev, T. Dieckmann, Thermodynamics and Kinetics of Adaptive Binding in the Malachite Green RNA Aptamer, Biochemistry. 52 (2013) 6575–6583. https://doi.org/10.1021/bi400549s.

[18] D.J. Patel, A.K. Suri, F. Jiang, L. Jiang, P. Fan, R.A. Kumar, S. Nonin, [1] D.J. Patel, A.K. Suri, F. Jiang, L. Jiang, P. Fan, R.A. Kumar, S. Nonin, Structure, recognition and adaptive binding in RNA aptamer complexes, J. Mol. Biol. 272 (1997) 645–664. https://doi.org/10.1006/jmbi.1997.1281.Structure, recognition and adaptive, J. Mol. Biol. 272 (1997) 645–664. https://doi.org/10.1006/jmbi.1997.1281.

[19] J. Flinders, S.C. DeFina, D.M. Brackett, C. Baugh, C. Wilson, T. Dieckmann, Recognition of Planar and Nonplanar Ligands in the Malachite Green-RNA Aptamer Complex, ChemBioChem. 5 (2004) 62–72. https://doi.org/10.1002/cbic.200300701.

[20] T. Dieckmann, E. Suzuki, G.K. Nakamura, J. Feigon, Solution structure of an ATP-binding RNA aptamer reveals a novel fold, RNA. 2 (1996) 628–640. https://doi.org/10.2210/pdb1raw/pdb.